Engineering Science and Technology, an International Journal 19 (2016) 1593–1599

HOSTED BY

ELSEVIER

Contents lists available at ScienceDirect

Engineering Science and Technology, an International Journal

journal homepage: www.elsevier.com/locate/jestch

Full Length Article

Mechanical properties, wear and corrosion behavior of copper matrix composites reinforced with steel machining chips

Kenneth Kanayo Alaneme *, Benjamin Ufuoma Odoni

Department of Metallurgical and Materials Engineering, Federal University of Technology, Akure PMB 704, Nigeria

ARTICLE INFO

Article history:
Received 15 February 2016
Revised 21 April 2016
Accepted 24 April 2016
Available online 7 June 2016

Keywords:
Copper matrix composites
Corrosion behavior
Interface bonding
Mechanical properties
Steel machining chips
Wear

ABSTRACT

The mechanical properties, wear and corrosion behavior of copper matrix composites reinforced with steel machining chips was investigated in this research. Steel machining chips with chip size range of 105 μm and below were utilized to develop stir cast copper matrix composites having 5, 7.5 and 10 wt % of the chips as reinforcement. Unreinforced copper and 10 wt% alumina reinforced copper matrix composites were also prepared for control experimentation. Hardness and tensile properties evaluation, wear test, potentiodynamic polarization corrosion tests, and optical microscopy; were used as basis to characterize the composites produced. The results show that the addition of steel machining chips in copper resulted in significantly low porosity levels in the copper matrix composites compared with the use of alumina as reinforcement. The mechanical properties (hardness and tensile properties) and wear resistance were also observed to improve with the use of the steel machining chips as reinforcement. The corrosion susceptibility in 3.5 wt% NaCl solution were observed to be more intense for the unreinforced copper and the alumina reinforced composite grade compared with the steel chips reinforced copper matrix composites. But in 0.3 M H_2SO_4 solution, no consistent corrosion trend was observed although the corrosion resistances of all the composite grades produced were superior to the unreinforced copper. The results demonstrate the capacity of steel machining chips to serve as a reliable cost effective and technically efficient reinforcement material for the development of copper matrix composites.

1. Introduction

Many applications within the electronic and manufacturing industries require components to be made with materials possessing high electrical and thermal conductivity, high corrosion and oxidation resistance as well as good mechanical properties [1,2]. This is in addition to maintaining microstructural stability and high temperature resistance [3]. For such applications requiring these highlighted spectrums of properties, copper matrix composites have been found to be the most promising engineering material for selection [4]. Specifically, copper matrix composites have been used for the design of radiators, electronic contact devices, casing of jet engines and in recent years as substitute materials for the design of cylinder heads, liners and brake discolor in automotive industry [3,5,6].

The development of copper matrix composites has relied on the use of ceramic reinforcements with alumina and silicon carbide the most commonly utilized [7–12]. The choice of both ceramic materials is largely influenced by their high hardness and wear resistances, refractory nature, and relative availability and cost advantage [13–15]. However, copper has been observed to exhibit very poor wetting for ceramic materials (alumina and silicon carbide inclusive) which often result in poor adhesion and interface strength between copper and ceramic reinforcement. The poor interface bonding adversely affects mechanical properties (strength) as it diminishes load transfer from the matrix to the stronger ceramic particles [4]; it has also been reported to affect adversely the physical properties of the composites [16,17].

Several efforts have been made to improve the interface bonding between copper and ceramic particles by exploring surface coating of the ceramic particles [17], and the use of alternative reinforcing materials such as carbon based graphite and graphene [18,19]. Efforts made with the use of graphite and graphene for instance have not adequately addressed the problem of weak copper/reinforcement bonding [4,19]. Also the use of graphene or the pre-coating of ceramic particles requires the use of more complex process technologies [20,21].

* Corresponding author.
E-mail address: kalanemek@yahoo.co.uk (K.K. Alaneme).
Peer review under responsibility of Karabuk University.

http://dx.doi.org/10.1016/j.jestch.2016.04.006

The poor wetting of ceramic materials by copper motivated the consideration of a metal based reinforcement in this research as copper is reported to have relatively good wettability for metals compared to ceramics [22]. In this regards, the use of pearlitic steels and stainless steels as reinforcement in copper has been reported with very significant improvement in mechanical properties recorded [23–25]. The specific choice of steel machining chips as reinforcement in this research was based on economic, environmental and metallurgical considerations. Steel machining chips is an industrial waste with no cost implications to acquire it from machining shops. Currently it has little well known direct use, and disposal or recycling of the steel chips has been a challenge in most developing countries. The mechanics of machining enlightens us that the high strain deformation underlying chip formation causes chip microstructures to be ultrafine grained [26,27]. The ultrafine microstructure imparts significantly high strength on the chips several orders of magnitude higher than that of the bulk material (could be well above 50–100%) [27,28]. It thus has the potential of improving the strength of a relatively softer matrix through load transfer from the matrix if good interface adhesion exists between the dispersed chips and the matrix.

It should be noted that the use of steel machining chips as reinforcements in metal matrix composites (MMCs) at present has attracted very little interest. The present work evaluates the mechanical properties, corrosion and wear behavior of copper matrix composites reinforced with steel machining chips.

2. Materials and method

2.1. Materials

The materials used for this research work are commercial pure copper which served as matrix for the composites to be developed; analytical grade alumina with average particle size of 30 μm (in accordance with Alaneme and Aluko, [29]) and steel machining chips, which both served as reinforcements. The steel chips used were discontinuous chippings from the milling of medium carbon steel. Due to the irregularities in the geometries and dimension of the machining chips, sieving of the chips was performed and chip size range of 105 μm and below was utilized for the purpose of the composite development.

2.2. Composite production

The production of the copper matrix composites with steel machining chips and alumina (as control sample) as reinforcements was performed using double stir casting procedure reported by Alaneme and Adewale [30] and Vyas and Pandey [31]. Copper and the steel machining chips required to produce copper based composites having 5, 7.5, and 10 wt% steel chips as reinforcement were determined by charge calculations. Also the charge estimate of the amount of alumina required to produce 10 wt% alumina reinforced copper matrix composite (the control experimental composition) was determined following the same procedure. The steel machining chips and alumina particles were preheated separately at a temperature of 250 °C to eliminate dampness, improve wettability with the molten copper and to reduce temperature gradient between the reinforcement and the matrix. The copper was charged into a gas fired crucible furnace fitted with an external temperature probe. The charge was heated to a temperature of 1150 °C ± 30 °C (above the liquidus temperature of copper) to ensure the copper melts completely. The liquid copper was cooled in the furnace to a semi solid state at a temperature of about 920 °C. The preheated mild steel machining chips and alumina particles (in separate heats) were charged into the semi-solid melt at this temperature (920 °C) and stirred manually for 5 min. The semi-solid composite mixture was then super heated to 1200 °C ± 30 °C and stirred using an automated mechanical stirrer. The mechanical stirring was performed at 300 rpm for 7 min before casting into sand molds fitted with metallic chills. The sand molds prepared had two different cavities – a cylindrical rod shape for samples which were mechanically processed (cold rolled) before machining to final testing configuration and discolor shape samples for wear testing. The processing temperatures and stirring times were selected based on knowledge of copper melting and solidification behavior, and processing factors as reported by Vyas and Pandey [31].

2.3. Cold rolling and heat treatment of samples

A miniature cold rolling machine with capability for rolling of flat and cylindrical profiles was utilized for the cold deformation processing. The as-cast composite grades produced in form of cylindrical rods were firstly machined to 12 mm diameter and 10 cm length, before homogenizing at 850 °C for 2 h. The samples were then cold rolled using the round grooves of the rolling machine from an initial diameter of 12 mm to a final diameter of 10.2 mm (15% cold rolling). The rods were cold deformed using six passes (translating to 0.25 mm reduction in diameter per pass) through the rolling dies until the final diameter of 10.2 mm was achieved. The cold rolling was done to reduce volume defects such as voids, blow holes and pores that may have developed during casting [32]. The as-rolled samples were subsequently heat treated at 350 °C for 1 h and quenched in water to remove internal stresses which may have arisen during the cold rolling process.

2.4. Composite density and percentage porosity

The experimental density of each grade of composite produced was determined by dividing the measured weight of a test sample by its measured volume using a digital weighing balance with tolerance of ±0.0001; while the theoretical density was evaluated by using the formula:

$$\rho\mathrm{Cu}/\textit{steel chips} = \mathrm{wt.Cu} \times \rho\mathrm{Cu} + \mathrm{wt.}\textit{steel chips} \times \rho\textit{steel chips} \tag{2.1}$$

$$\rho\mathrm{Cu}/\mathrm{Al_2O_3} = \mathrm{wt.Cu} \times \rho\mathrm{Cu} + \mathrm{wt.Al_2O_3} \times \rho\mathrm{Al_2O_3} \tag{2.2}$$

where ρCu/*steel chips* = density of steel chips reinforced Cu matrix Composite, wt. Cu = weight fraction of Cu, ρCu = density of Cu, wt. *steel chips* = weight fraction steel chips, ρ*steel chips* = density of steel chips, wt. Al_2O_3 = weight fraction Al_2O_3, and ρAl_2O_3 = density of Al_2O_3.

The experimental densities were compared with the theoretical densities for each composition of the composites produced; and it served as basis for evaluation of the percent porosity of the composites using the relations [30]:

$$\%\mathrm{porosity} = \frac{(\rho T - \rho EX)}{\rho T} \times 100\% \tag{2.3}$$

where, ρT represents theoretical density (g/cm^3), and ρEX represents experimental density (g/cm^3).

2.5. Mechanical testing

Hardness testing and tensile properties evaluation were used to assess the mechanical properties of the composites produced. The hardness of the composites produced was evaluated on a hardness testing machine using the Rockwell hardness "C" scale. Specimens cut out from each composite composition were representative of

the bulk samples and polished to obtain a smooth plane parallel surface for proper hardness indentation. Seven hardness indents were made on each specimen and readings within the margin of ±2% were taken for the computation of the average hardness values of the specimens.

The tensile properties of the composites were evaluated at room temperature using an Instron universal testing machine. The test was conducted at a strain rate of 10^{-3}/s using specimens with dimensions 5 mm diameter and 30 mm gauge length in accordance with Alaneme and Sanusi [33]. The specimen configuration, testing procedure and basis for determination of the tensile properties were in accordance with the specifications of ASTM E8M-04 [34] standard.

2.6. Microstructural examination

Optical microscopy was used for microstructural characterization of the composites produced. The samples for examination were prepared to metallographic finish using a series of grinding and polishing operations. The samples were etched by swabbing for 20 s using an etching solution containing 30 cm^3 of HCl and 10 g FeCl. A JSM 7600F Jeol ultra-high resolution field emission gun scanning electron microscope (FEG-SEM) equipped with an EDS was also used for detailed study of the microstructural features and qualitative elemental composition of the composites produced.

2.7. Wear behavior

The wear behavior of the composites was evaluated using a rotary platform abrasion tester commonly referred to as the Taber abrasion machine. The discolor shaped composite grades produced were machined to 200 mm diameter and 6 mm thickness in accordance with the specification for wear test using the Taber abrasion machine [33]. The samples were placed on the turntable platform of the wear machine and gripped at a constant pressure by two abrasive wheels lowered onto the sample surface. In operation, the turntable rotates with the sample which drives the abrasive wheels in contact with its surface. The rubbing action between the sample and the abrasive wheel during the rotating motion of the machine, results in the generation of loose composite debris from the sample surface. The initial weight and final weight of the samples were measured using digital weighing balance, and the wear index calculated using the relation [33]:

$$\text{Wear Index(W.I)} = \frac{(\textit{Intial weight} - \textit{final weight}) \times 1000}{\textit{time of testcycle}} \qquad (2.4)$$

where the initial and final weights were measured in grammes, and the time of wear test cycle measured in minutes. The Taber Abrasion machine utilized for the wear testing is presented in Fig. 1.

Fig. 1. Taber abrasion machine utilized for wear testing of the composites produced.

2.8. Corrosion behavior

Corrosion testing was conducted using potentiodynamic polarization electrochemical methods in accordance with ASTM G5-94 [35] standard. Corrosion behavior of the samples was investigated in 0.3 M H_2SO_4 and 3.5 wt% NaCl solutions at room temperature (25 °C) using an AutoLAb potentiostat. Potentiodynamic polarization measurements were carried out using a scan rate of 1.0 mV/s at a potential initiated at −200 mV to +250 mV. Three repeat tests were carried out for all compositions of the composites to guarantee the reproducibility and repeatability of results from the triplicates. The surface morphology of the composites after immersion in the corrosion solutions was assessed using the JSM 7600F Jeol ultra-high resolution field emission gun scanning electron microscope (FEG-SEM).

3. Results and discussion

3.1. Microstructure

Fig. 2 shows representative SEM micrograph and EDS profile of the 5 wt% steel chips reinforced composite produced. The microstructure shows color contrast (dark and bright fields) in the copper matrix with visible dispersion of the reinforcing particulates (Fig. 2a). The light phase is the copper matrix while the dark phase show different size and morphology of the discontinuously formed (type I) steel machining chips used as reinforcement for the composite production. The microstructural features observed were similar to that of other composite grades produced, hence its selection as representative for all grades. The EDS profile (Fig. 2b) shows peaks of copper (Cu), iron (Fe) and carbon (C), confirming the presence of the steel chips dispersed in the copper matrix.

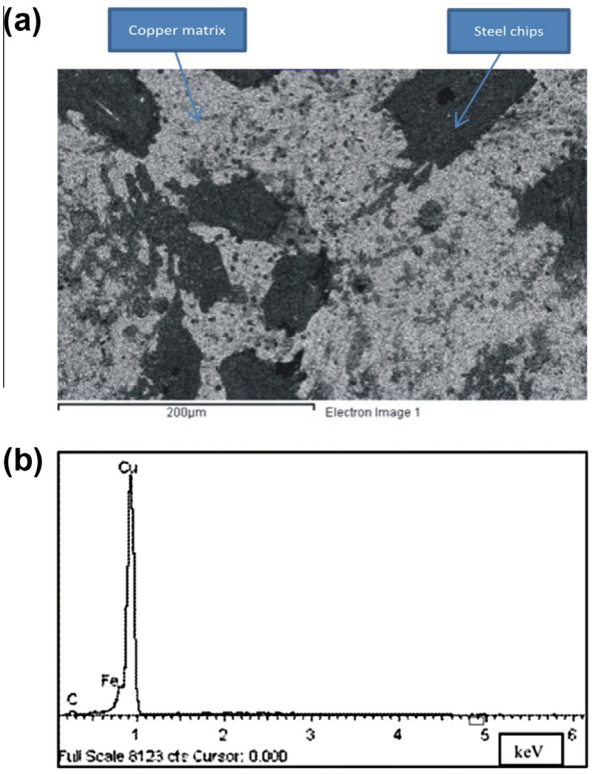

Fig. 2. (a) Representative SEM micrograph of the copper matrix composite reinforced with 5 wt% steel machining chips (b) EDS profile of the copper matrix composite reinforced with 5 wt% steel machining chips.

3.2. Composite densities and percent porosities

Table 1 shows the densities and percent porosities in the composites produced. It is observed that the composite densities are generally lower than that of the unreinforced copper, and the density decreases with increase in the weight percent of the steel machining chips. This is expected as the density of steel (7.6 g/cm^3) is lower than that of copper (8.96 g/cm^3). The percent porosity in the composites is however observed to increase with increase in the weight percent of the steel chips. It should be noted that the maximum porosity level of less than 2.2% was obtained for the 10 wt% steel chips reinforced copper matrix composites. For the alumina reinforced composite grade, the percent porosity was 3.78% close to twice the maximum percent porosity observed for the most porous of the steel chips reinforced composites. This relatively higher percent porosity in the alumina reinforced composite can be linked to the poor wetting between copper and ceramic particles (alumina) which easily results in the generation of pores mainly in the matrix/reinforcement interfaces. This condition is reported to be largely responsible for lower mechanical and wear properties in copper matrix composites reinforced with ceramics [4].

3.3. Mechanical properties

Fig. 3 shows the hardness of the different compositions of the composites produced. The hardness of the copper matrix composites is observed to increase with increase in the weight percent of steel machining chips. The hardness of the alumina reinforced copper composite grade which served as the control sample had hardness value slightly lower than that of the steel chips reinforced composite grades. This can be linked to the relatively higher percent porosity of the alumina reinforced copper composites compared with the composite grades reinforced with the steel machining chips. Representative tensile properties of the composites produced derived from the stress–strain curves (Fig. 4) are presented in Table 2. It is observed that the 5 wt% steel machining chips reinforced copper composite grade has superior ultimate tensile strength, percent elongation, and tensile toughness compared to the control samples (unreinforced copper and 10 wt% alumina reinforced copper matrix composite). The increase in strength is reasoned to be on account of the strong interface bonding between the copper matrix and the steel machining chips which allows for the transfer and distribution of load from the matrix to the reinforcement. Also improved ductility is linked to higher plastic strain sustaining capacity which is significantly enhanced by good matrix/reinforcement interface bonding [17]. From these results it can therefore be said that the incorporation of steel machining chips as reinforcement in copper matrix composites holds promise for improved mechanical properties.

3.4. Wear behavior

The wear test results for the composites produced are presented in Fig. 5. It is observed that the wear index (a measure of wear rate) increases with increase in the weight percent of the steel machining chips but most intense for the alumina reinforced copper matrix composite. This again shows that the steel machining chips can serve as reinforcement in copper matrix composites for wear resistance applications. The high wear rate observed in the alumina reinforced copper matrix composites can be tied to the relatively high porosity levels and poor matrix/alumina particulate interface bonding which facilitate the abrasive wear of the composite. Similar wear pattern was reported in ZnAl based composites reinforced with steel machining chips by Iglesias et al. [28]; where it is reported that a high integrity interface formed between the metallic matrix (Zn-Al based alloy) and the steel chips, prevents chip pullout and damage during wear.

Table 1
Composite densities and percent porosities of the unreinforced copper and copper metal matrix composites produced.

Sample composition	Theoretical density (g/cm^3)	Experimental density (g/cm^3)	Porosity (%)
Unreinforced copper	8.96	8.840	1.34
Cu-5 wt% steel chips	8.9045	8.805	1.12
Cu-7.5 wt% steel chips	8.8768	8.775	1.15
Cu-10 wt% steel chips	8.849	8.655	2.19
Cu-10 wt% Al_2O_3	8.459	8.139	3.78

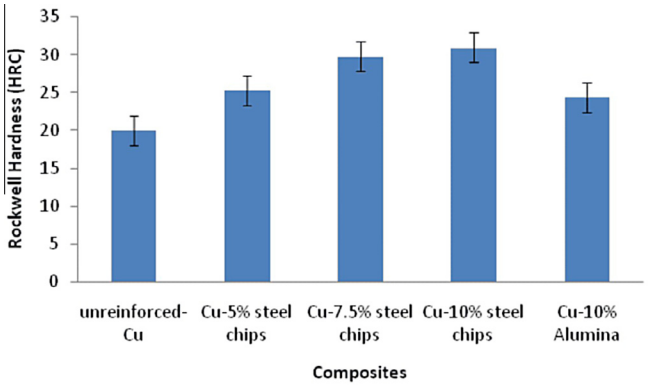

Fig. 3. Rockwell hardness results of the unreinforced copper and copper matrix composites produced.

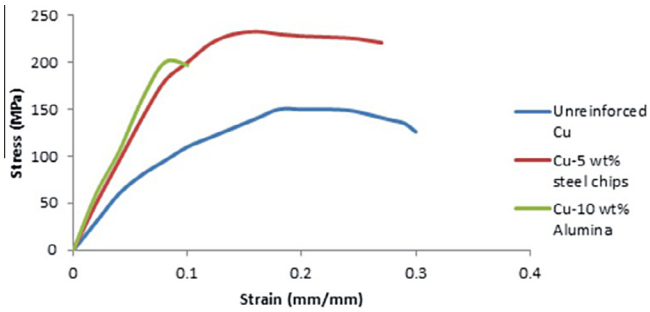

Fig. 4. Representative stress–strain plots of the composites.

Table 2
Tensile properties of the unreinforced copper and selected composites produced.

Sample composition	UTS (MPa)	Elongation (%)	Tensile toughness (J/m^3)
Unreinforced copper	150 ± 4	30 ± 1.2	10 ± 0.5
Cu-5 wt% Steel chips	235 ± 5.5	27 ± 0.8	29 ± 0.4
Cu-10 wt% Al_2O_3	200 ± 6	10 ± 1.0	8 ± 0.6

3.5. Corrosion behavior

Potentiodynamic polarization curves of the unreinforced copper and copper matrix composites produced in 3.5 wt% NaCl solution is presented in Fig. 6. From Fig. 6, it is observed that the composites exhibited similar polarization and passivity characteristics. However, the corrosion current densities (Icorr) and corrosion potentials (Ecorr) indicate clear distinct corrosion behavior between the steel chips reinforced composite series and the unreinforced

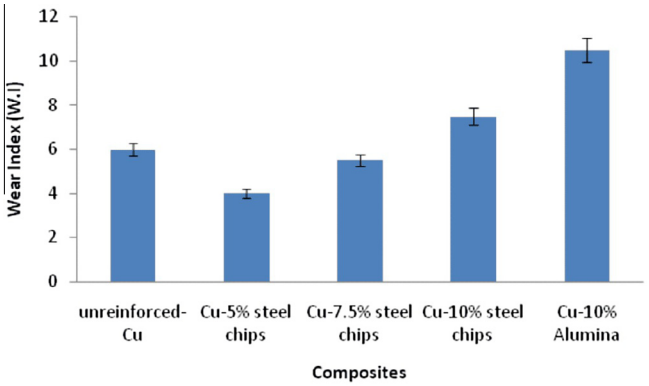

Fig. 5. Wear index of the unreinforced copper and copper matrix composites produced.

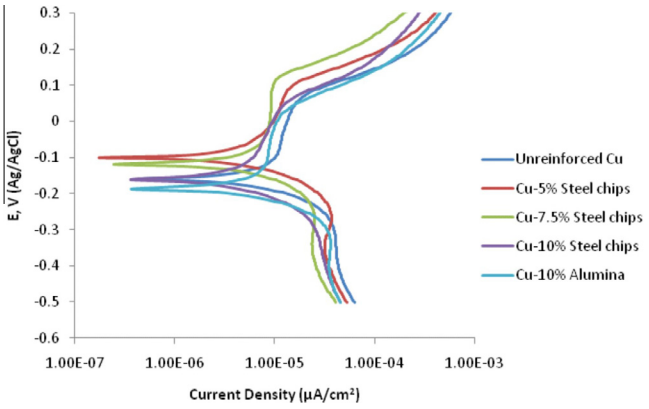

Fig. 6. Potentiodynamic polarization curves of the unreinforced copper and copper matrix composites produced in 3.5 wt% NaCl solution.

copper and alumina reinforced copper matrix composite grade (Table 3). It is observed from Table 3 that the corrosion current densities were more intense for the unreinforced copper and the alumina reinforced composite grade in comparison with the steel chips reinforced copper matrix composites. This indicates that the steel chips reinforced copper matrix composites are more resistant to corrosion in 3.5 wt% NaCl solution. The Icorr values of the steel chips reinforced copper matrix composites are observed to be within the same range that is the corrosion resistances of the samples are basically at the same level. The Ecorr values are supportive of the Icorr trends as it is observed that the steel chips reinforced composites have higher corrosion potentials compared with the unreinforced copper and alumina reinforced copper matrix composite. The Ecorr trend was more consistent in the steel chips reinforced copper matrix composites as it is observed to decrease slightly with increase in wt% steel chips; but generally higher than that of the unreinforced and alumina reinforced composite grade. This indicates that the steel chips reinforced copper matrix composites have a lower thermodynamic tendency to corrode in 3.5 wt% NaCl solution compared to the unreinforced and alumina reinforced copper matrix composite grade. That is the steel chips reinforced copper matrix composites are more thermodynamically stable in 3.5 wt% NaCl solution.

Fig. 7 shows the SEM image and EDS profile of the surface morphology of a representative sample of the steel chips reinforced copper matrix composite (the 5 wt% steel chips reinforced copper matrix composite) after the electrochemical test in 3.5 wt% NaCl solution. The structure (Fig. 7a) is observed to have numerous pores initiated in the copper matrix. There is no clear indication

Table 3
Electrochemical data for the unreinforced copper and the copper matrix composites produced in 3.5 wt% NaCl solution.

Sample	Ecorr (V)	Icorr (μA/cm^2)
Unreinforced copper	−0.16	3.172
Cu-5% steel chips	−0.101	2.057
Cu-7.5% steel chips	−0.118	2.118
Cu-10% steel chips	−0.161	1.922
Cu-10% Al_2O_3	−0.186	2.996

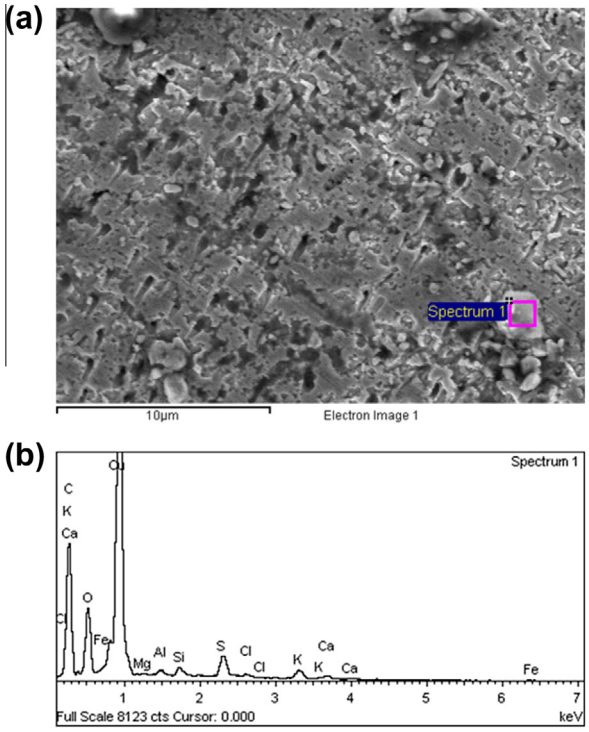

Fig. 7. SEM characterization of the 5 wt% steel chips reinforced copper matrix composite showing (a) secondary electron imaging of the surface after electrochemical testing in 3.5 wt% NaCl solution, and (b) EDS profile of the surface morphology of the corroded sample.

that these pores are initiated on the sites of the steel chips (considering the small size of the pores in comparison with that of the steel chips used in this research) or showed preference to occur at the copper/steel machining chips interface. Bakkar and Ataya [36] observed similar corrosion surface morphology in stainless steel fiber reinforced copper matrix composites electrochemically studied in NaCl environment. They reported that corrosion of the stainless steel reinforced copper matrix composites in chloride media began at the copper matrix at sites independent of the stainless steel fibers or stainless steel/copper interface. They noted that pitting of the stainless steel fibers only appeared much later. This they held was a good indication of sound bonding at the interface between the stainless steel fibers and the copper matrix. The EDS profile (Fig. 7b) confirms the presence of the chlorine which is the halide ion present in NaCl solution.

Fig. 8 shows the potentiodynamic polarization curves for the unreinforced copper and copper matrix composites produced in 0.3 M H_2SO_4 solution. Apart from the 7.5 wt% steel chips reinforced copper matrix composite with polarization curves depressed to relatively lower potentials, it is observed that the other composite grades and the unreinforced copper exhibited similar polarization and passivity characteristics. From Table 4, it is observed that the 7.5 wt% steel chips reinforced copper matrix composite had the

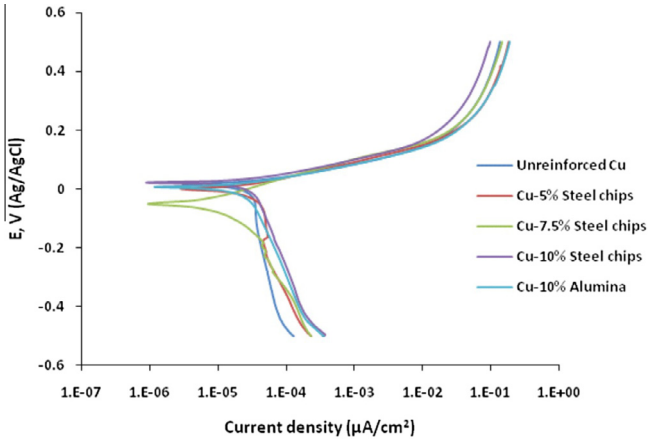

Fig. 8. Potentiodynamic polarization curves of the unreinforced copper and copper matrix composites produced in 0.3 M H_2SO_4 solution.

Table 4
Electrochemical data for the unreinforced copper and the copper matrix composites produced in 0.3 M H_2SO_4 solution.

Sample	Ecorr (V)	Icorr (μA/cm^2)
Unreinforced copper	0.160	7.979
Cu-5% steel chips	0.001	5.040
Cu-7.5% steel chips	−.490	1.739
Cu-10% steel chips	.024	6.063
Cu-10% Al_2O_3	.007	4.862

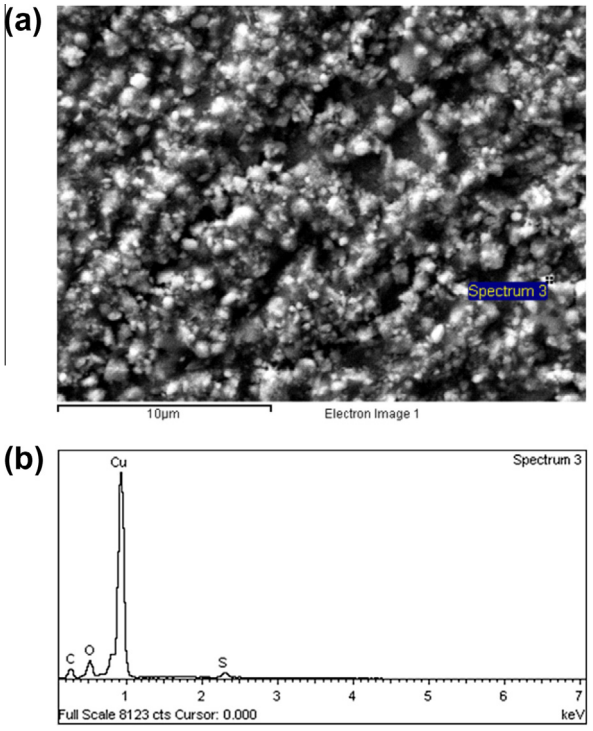

Fig. 9. SEM characterization of the 7.5 wt% steel chips reinforced copper matrix composite showing (a) secondary electron image of the surface after electrochemical testing in 0.3 M H_2SO_4 solution, and (b) EDS profile of the surface morphology of the corroded sample.

least Icorr value suggesting that it is the least susceptible to corrosion in 03 M H_2SO_4 solution. It is also observed that all the steel chips reinforced copper matrix composite grades and the alumina reinforced copper composite had Icorr values lower than that of the unreinforced copper. The alumina reinforced copper matrix composite is observed to exhibit slightly lower icorr values compared to the 5 and 10 wt% steel chips reinforced composites. The corrosion resistance of the composites in this medium (0.3 M H_2SO_4 solution) clearly did not follow a consistent pattern but distinctively shows that all the composite grades have superior corrosion resistance to the unreinforced copper. The Ecorr values show that corrosion potential of the 5 and 10 wt% steel chips reinforced copper matrix composites and the 10 wt% alumina reinforced copper matrix composite grade are within the same range. This is an indication of comparable level of thermodynamic stability of the composites in 0.3 M H_2SO_4 solution compared to that of the unreinforced copper.

Fig. 9 shows the SEM image of the surface morphology of a representative sample of the steel chips reinforced copper matrix composite (the 7.5 wt% steel chips reinforced copper matrix composite) after the electrochemical test in 0.3 M H_2SO_4 solution. The surface morphology of the sample (Fig. 9a) show corrosion products on the surface of the composites which are most likely copper oxide variants as suggested by the EDS profile (Fig. 9b) which show peaks of Cu, S, and O. The observations by Bakkar and Ataya [36] seem to give credence to this position although their study was in acidic NaCl solution. They noted that in this environment, the nature of corrosion in stainless steel reinforced copper matrix composites is characterized by microgalvanic corrosion with the reversal of the cell anode between the stainless steel fibers and the copper matrix. That is at the beginning, stainless steel served as the anode in the galvanic couple with copper. The role was however reversed after a short time with copper acting as the cell anode, thereby making the galvanic couple system of copper/stainless steel to have equilibrium polarity in which copper is anode in all conditions studied. This same scenario may have played out in the steel chips reinforced copper matrix composites in which case preferential dissolution of the steel chips from the copper matrix was surprisingly not the observed corrosion mechanism.

4. Conclusion

The mechanical properties, wear and corrosion behavior of copper matrix composites reinforced with steel machining chips has been investigated. The results have shown clearly that steel machining chips can serve as a cost effective and technically reliable reinforcement for the development of copper matrix composites. Specifically:

1. The addition of steel machining chips in copper was found to result in very low porosity level in the copper matrix composites compared with the use of alumina as reinforcement.
2. The mechanical properties (hardness and tensile properties) and wear resistance were also observed to improve with the use of the steel machining chips as reinforcement similar to observations made by Grunberger et al. [24] and Hamada et al. [25].
3. The corrosion susceptibility in 3.5 wt% NaCl solution were more intense for the unreinforced copper and the alumina reinforced composite grade compared with the steel chips reinforced copper matrix composites. But in 0.3 M H_2SO_4 solution, no consistent corrosion trend was observed although the corrosion resistance of all the composite grades produced were superior to the unreinforced copper.
4. Pitting was initiated in the copper matrix in 3.5 wt% NaCl solution with no clear indication that the pits were initiated preferentially on the sites of the steel chips or at the copper matrix/

steel machining chips interface. In 0.3 M H_2SO_4 solution, corrosion products were observed on the surface of the composites which are thought to be copper oxide variants, suggesting that copper was anodic to the steel chips in the medium.

5. The corrosion mechanisms for both corrosive media followed similar trends in stainless steel fiber reinforced copper matrix composites reported by Bakkar and Ataya [36].

References

[1] A. Molina, A. Torres-Islas, S. Serna, M. Acosta-Flores, R.A. Rodriguez-Diaz, J. Colin, Corrosion, electrical and mechanical performance of copper matrix composites produced by mechanical alloying and consolidation, Int. J. Electrochem. Sci. 10 (2015) 1728–1741.

[2] R. Zitoune, M. El Mansori, K. Vijayan, Tribo-functional design of double cone drill implications in tool wear during drilling of copper mesh/CFRP/woven ply, Wear 302 (1–2) (2013) 1560–1567.

[3] S. Mallik, N. Ekere, C. Best, R. Bhatti, Investigation of thermal management materials for automotive electronic control units, Appl. Therm. Eng. 31 (2011) 355–362.

[4] S. Kumari, A. Kumar, P.R. Sengupta, P.K. Dutta, R.B. Mathur, Improving the mechanical and thermal properties of semi-coke based carbon/copper composites reinforced using carbon nanotubes, J. Adv. Mater. Lett. 5 (5) (2014) 265–271.

[5] J. Dutkiewicz, P. Ozga, W. Maziarz, J. Pstrus, B. Kania, P. Bobrowski, et al., Microstructure and properties of bulk copper matrix composites strengthened with various kinds of graphene nanoplatelets, Mater. Sci. Eng., A 628 (2015) 124–134.

[6] G.C. Efe, T. Yener, I. Altinsoy, M. Ipek, S. Zeytin, C. Bindal, The effect of sintering temperature on some properties of Cu–SiC composite, J. Alloys Compd. 509 (2011) 6036–6042.

[7] R. Sathiskumar, N. Murugan, I. Dinaharan, S.J. Vijay, Fabrication and characterization of Cu/B4c surface dispersion strengthened composite using friction stir processing, Arch. Met. Mater. 59 (2014) 83–89.

[8] W.V. Sagar, S.L. Samir, W.R. Amit, Modelling of Cu-Al_2O_3 metal matrix composite prepared by powder metallurgy route, Int. J. Eng. Adv. Technol. 3 (2013) 330–332.

[9] M. Yusoff, R. Othman, Z. Hussain, Mechanical alloying and sintering of nanostructured tungsten carbide-reinforced copper composite and its characterization, Mater. Des. 32 (2011) 3293–3298.

[10] Q. Kang, X. He, S. Ren, L. Zhang, M. Wu, C. Guo, W. Cui, X. Qu, Preparation of copper–diamond composites with chromium carbide coatings on diamond particles for heat sink applications, Appl. Therm. Eng. 60 (2013) 423–429.

[11] L. Zhang, X.H. Qu, X.B. He, B.H. Duan, S.B. Ren, M.L. Qin, Thermo-physical and mechanical properties of high volume fraction SiCp/Cu composites prepared by pressureless infiltration, Mater. Sci. Eng., A 489 (2008) 285–293.

[12] B.M. Girish, B.R. Basawaraj, B.M. Satish, D.R. Somash, Electrical resistivity and mechanical properties of tungsten carbide reinforced copper alloy composites, Int. J. Comput. Mater. 2 (3) (2012) 37–42.

[13] V. Aleksandar, R. Viseslava, Z. Fatima, Friction and wear properties of copper based composites reinforced with micro and nano-sized Al_2O_3 particles, 8th Int. conf. Tribol., 30th Oct-1st Nov. 2014, Sinaia, Romania, 2014, pp. 357–358.

[14] A.A. Thakre, S. Soni, Modeling of burr size in drilling of aluminum silicon carbide composites using response surface methodology, Eng. Sci. Technol. 19 (2016) 1199–1205.

[15] I. Dinaharan, N. Murugan, A. Thangarasu, Development of empirical relationships for prediction of mechanical and wear properties of AA6082 aluminum matrix composites produced using friction stir processing, Eng. Sci. Technol. 19 (2016) 1132–1144.

[16] S.F. Moustafa, Z. Abdel-Hamid, A.M. Abd-Elahi, Copper matrix SiC and Al_2O_3 particulate composites by powder metallurgy technique, Mater. Lett. 53 (2002) 244–249.

[17] J. Li, H. Zhang, Y. Zhang, Z. Che, X. Wang, Microstructure and thermal conductivity of Cu/diamond composites with Ti-coated diamond particles produced by gas pressure infiltration, J. Alloy. Compd. 647 (2015) 941–946.

[18] J. Kovacik, S. Emmer, J. Bielek, Thermal conductivity of Cu–graphite composites, Int. J. Therm. Sci. 90 (2015) 298–302.

[19] F. Chen, J. Ying, Y. Wang, S. Du, Z. Liu, Q. Huang, Effects of graphene content on the microstructure and properties of copper matrix composites, Carbon 96 (2016) 836–842.

[20] W. Yang, L. Zhou, K. Peng, J. Zhu, L. Wan, Effect of tungsten addition on thermal conductivity of graphite/copper composites, Compos. Part B Eng. 55 (2013) 1–4.

[21] H. Zhang, M. Chao, H. Zhang, A. Tang, B. Ren, X. He, Microstructure and thermal properties of copper matrix composites reinforced by chromium-coated discontinuous graphite fibers, Appl. Therm. Eng. 73 (2014) 739–744.

[22] D.D. Gu, Y.F. Shen, Z.J. Lu, Microstructural characteristics and formation mechanism of direct laser-sintered Cu-based alloys reinforced with Ni particles, Mater. Des. 30 (2009) 2099–2107.

[23] W. Grünberger, M. Heilmaier, L. Schultz, High-strength pearlitic steel–copper composite wires for conductors in pulsed high-field magnets, Mater. Sci. Eng., A 303 (1–2) (2001) 127–133.

[24] W. Grünberger, M. Heilmaier, L. Schultz, High-strength, high-nitrogen stainless steel–copper composite wires for conductors in pulsed high-field magnets, Mater. Lett. 52 (3) (2002) 154–158.

[25] A.S. Hamada, A. Khosravifard, A.P. Kisko, E.A. Ahmed, D.A. Porter, High temperature deformation behavior of a stainless steel fiber-reinforced copper matrix composite, Mater. Sci. Eng., A (2016), http://dx.doi.org/10.1016/j.msea.2016.03.084.

[26] C. Saldana, S. Swaminathan, T.L. Brown, W. Moscoso, J.B. Mann, W.D. Compton, S. Chandrasekar, Unusual applications of machining: controlled nanostructuring of materials and surfaces, ASME J. Manuf. Sci. Eng. 132–3 (2010) 030908.

[27] T.L. Brown, S. Swaminathan, S. Chandrasekar, W.D. Compton, A.H. King, K.P. Trumble, Low-cost manufacturing process for nanostructured metals and alloys, J. Mater. Res. 17 (10) (2002) 2484–2488.

[28] P. Iglesias, A.E. Jiménez, M.D. Bermúdez, B.C. Rao, S. Chandrasekar, Steel machining chips as reinforcements to improve sliding wear resistance of metal alloys: study of a model Zn-based alloy system, Tribol. Int. 65 (2013) 215–227.

[29] K.K. Alaneme, A.O. Aluko, Production and age-hardening behaviour of Borax pre-mixed SiC reinforced Al–Mg–Si alloy composites developed by double stir casting technique, West Indian J. Eng. 34 (1/2) (2012) 80–85.

[30] K.K. Alaneme, T.M. Adewale, Influence of rice husk ash–silicon carbide weight ratios on the mechanical behaviour of Al–Mg–Si alloy matrix hybrid composites, Tribol. Ind. 35 (2) (2013) 163–172.

[31] T.K. Vyas, A. Pandey, A review on investigation of copper matrix composite by using stir casting method, Indian J. Appl. Res. 5 (1) (2015) 75–77.

[32] K.K. Alaneme, Influence of thermo-mechanical treatment on the tensile behaviour and CNT evaluated fracture toughness of borax premixed silicon carbide reinforced aluminium (6063) matrix composites, Int. J. Mater. Mech. Eng. 7 (1) (2012) 96–100.

[33] K.K. Alaneme, K.O. Sanusi, Mechanical and wear behaviour of rice husk ash–alumina–graphite hybrid reinforced aluminium based composites, Eng. Sci. Technol. Int. J. 18 (3) (2015) 416–422.

[34] ASTM E8M-04, Standard Test Methods for Tension Testing of Metallic Materials [Metric], ASTM International, West Conshohocken, 2004.

[35] ASTM G5-14, Standard Reference Test Method for Making Potentiostatic and Potentiodynamic Anodic Polarization Measurements, ASTM International, West Conshohocken, 2014.

[36] A. Bakkar, S. Ataya, Corrosion behaviour of stainless steel fibre-reinforced copper metal matrix composite with reference to electrochemical response of its constituents, Corros. Sci. 85 (2014) 343–351.